Proc. Natl. Acad. Sci. USA
Vol. 93, pp. 7618–7622, July 1996
Biophysics

Sequence-specific recognition by cytosine C^5 and adenine N^6 DNA methyltransferases requires different deformations of DNA

RICARDO A. GARCÍA*, CARLOS J. BUSTAMANTE†, AND NORBERT O. REICH*

*Department of Chemistry and Program in Biochemistry and Molecular Biology, University of California, Santa Barbara, CA 93106; and †Howard Hughes Medical Institute, University of Oregon, Eugene, OR 97403

Communicated by Robert L. Sinsheimer, University of California, Santa Barbara, CA, March 25, 1996 (received for review December 8, 1995)

ABSTRACT **DNA methyltransferases modify specific cytosines and adenines within 2–6 bp recognition sequences. We used scanning force microscopy and gel shift analysis to show that M.*Hha*I, a cytosine C^5 DNA methyltransferase, causes only a 2° bend upon binding its recognition site. Our results are consistent with prior crystallographic analysis showing that the enzyme stabilizes an extrahelical base while leaving the DNA duplex otherwise unperturbed. In contrast, similar analysis of M.*Eco*RI, an adenine N^6 DNA methyltransferase, shows an average bend angle of approximately 52°. This distortion of DNA conformation by M.*Eco*RI is shown to be important for sequence-specific binding.**

Protein-mediated distortions of canonical B-DNA can contribute to DNA recognition, as demonstrated for the bacteriophage λ integration host factor (1), catabolite activator protein (2–4), and the TATA binding protein (5–7). For sequence-specific enzymes, such distortions may further contribute to the correct assembly of active site residues and provide access to specific DNA moieties. A comparison of DNA substrates derived from enzyme-DNA cocrystal structures (Fig. 1) reveals diverse enzyme-induced DNA conformations. An unprecedented example of enzyme-mediated alteration in DNA conformation was recently described for the *Hha*I cytosine C^5 DNA methyltransferase (M.*Hha*I), which modifies the DNA sequence GCGC at the first cytosine (11). The cocrystal structure of the covalent enzyme-DNA complex, obtained by incorporating a mechanism-based inhibitor in place of the target cytosine, clearly shows the cytosine analog to be extrahelical while the remaining DNA is in the B-DNA conformation (Fig. 1*D*). The resulting orientation of the target cytosine presumably facilitates access for subsequent chemical modification by the enzyme (11). The M.*Hha*I provides an alternative paradigm to the large-scale DNA conformational changes observed in other protein–DNA complexes; similar mechanisms have recently been suggested for exonuclease III (12), uracil–DNA glycosylase (13), and DNA photolyase (14). How other classes of methyltransferases modify their DNA is unknown.

We examined the M.*Hha*I and an adenine N^6 methyltransferase (M.*Eco*RI, GAATTC, modifies the underlined adenine) to determine how different classes of DNA methyltransferases affect DNA structure, and in particular, the extent to which these enzymes bend DNA. The M.*Hha*I consists of a 327-aa polypeptide folded into two domains; the DNA is bound into the intervening cleft with the major groove contacted exclusively through one protein domain, while the larger catalytic domain contains the cofactor binding site and faces the minor groove (11). The M.*Hha*I contains 10 conserved amino acid regions that appear in all cytosine C^5 DNA methyltransferases (15). Adenine N^6 DNA methyltransferases also show regions of conserved amino acid sequences, including a region involved in AdoMet binding also found in cytosine C^5 DNA methyltransferases (16). The M.*Eco*RI is a 326-aa polypeptide folded into two domains connected by a flexible hinge segment (17); this hinge forms part of the cofactor binding site (18). The M.*Hha*I and M.*Eco*RI both show significant conformational changes upon binding DNA (9, 17). These enzymes have similar catalytic turnover constants [M.*Hha*I, 1.3 min^{-1} (19); M.*Eco*RI, 8.5 min^{-1} (20)] and K_m^{DNA} values (M.*Hha*I, 2.3 nM; M.*Eco*RI, 0.35 nM), although the combined differences result in a significantly larger k_{cat}/K_m^{DNA} for the M.*Eco*RI (M.*Hha*I, 0.094×10^8 M^{-1} s^{-1}; M.*Eco*RI, 4.0×10^8 $M^{-1}{\cdot}s^{-1}$). Both enzymes can bind DNA in the absence of cofactor, but unlike the M.*Hha*I, the M.*Eco*RI requires the cofactor (or cofactor analog, sinefungin) for sequence-specific binding (21). Since neither enzyme shows processive catalysis (22, 23), these enzymes must dissociate from the DNA as the enzyme–*S*-adenosylhomocysteine complex subsequent to catalysis.

We used scanning force microscopy (SFM) and gel shift analysis to determine the extent to which both enzymes bend DNA. These complementary methods show that only M.*Eco*RI bends DNA, and this distortion of DNA conformation is important for sequence-specific DNA recognition. Thus, DNA recognition and modification by these enzymes requires different distortions of DNA.

MATERIALS AND METHODS

Materials. M.*Eco*RI was purified from *Escherichia coli* strain MM294 containing plasmid pDRCW (24). M.*Hha*I was generously provided by Sanjay Kumar (New England Biolabs). *Bam*HI and *Nhe*I endonucleases, Deep Vent DNA polymerase, T4 polynucleotide kinase, and 100 mM dNTP solutions were purchased from New England Biolabs, and calf intestinal alkaline phosphatase from Boehringer Mannheim. Plasmid pGEM-3 was purchased from Promega. DNA synthesis reagents were obtained from MilliGen/Biosearch. PCR primers were prepared on a Cyclone Plus DNA Synthesizer (Milligen/Biosearch) by solid phase β-cyanoethyl phosphoramidite chemistry and purified on Oligo-Pak (Waters) purification columns. [γ-^{32}P]ATP (6000 Ci/mmol; 1 Ci = 37 GBq) was purchased from Amersham. Sinefungin was obtained from Sigma.

DNA Substrates. DNA substrates were constructed by PCR amplification of pGEM-3 by using an MJ Research (Cambridge, MA) PCR Cycler (25). For circular permutation analysis of M.*Eco*RI, primers were designed to yield a set of DNA fragments 110 bp long containing a single *Eco*RI site located at varying distances from an end. The locations of the binding sites are shown in Fig. 2. In addition, two 300-bp DNA substrates with binding sites at the center or 12 bp from one end were constructed for bend angle measurements by the method of Thompson and Landy (26). Two DNA fragments for site-specific M.*Hha*I–DNA complexes were also con-

The publication costs of this article were defrayed in part by page charge payment. This article must therefore be hereby marked "*advertisement*" in accordance with 18 U.S.C. §1734 solely to indicate this fact.

Abbreviation: SFM, scanning force microscopy.

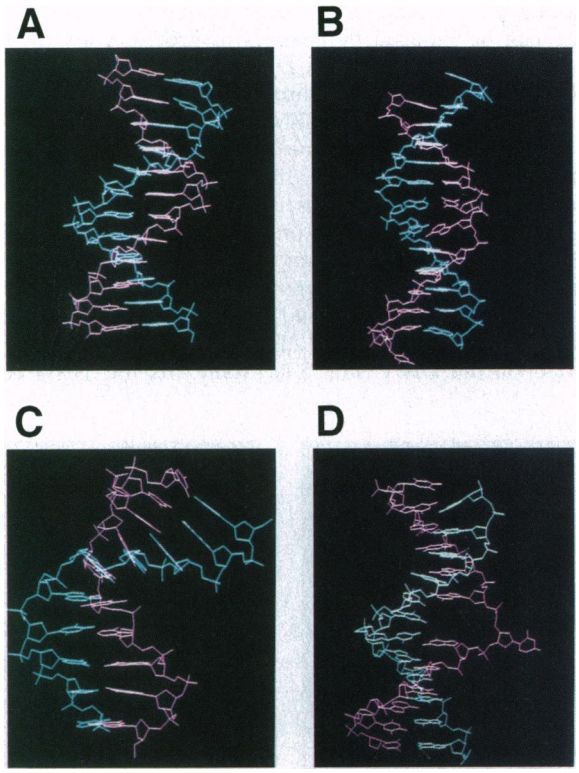

FIG. 1. DNA conformations within enzyme-DNA complexes. (*A*) Dickerson dodecamer (8). (*B–D*) Views of cocrystal DNAs of *Eco*RI endonuclease (9) (*B*), *Eco*RV endonuclease (10) (*C*), and *Hha*I cytosine C^5 DNA methyltransferase (11) (*D*).

structed by PCR amplification of plasmid pGEM-3 (*Hha*I site at position 1733). The 300-bp fragments contained a binding site located in the center or 12 bp from an end. PCR conditions consisted of 100 ng pGEM-3 as template, 1 μg of each specific primer, 200 μM of each dNTP, 10 mM KCl, 20 mM Tris·HCl (pH 8.8), 10 mM $(NH_4)_2SO_4$, 2 mM $MgSO_4$, 0.1% Triton X-100, and 2 units of Deep Vent DNA polymerase in a 100 μl reaction volume. The reactions were overlaid with 50 μl of mineral oil and subjected to 35 amplification cycles with the following profile: 1 min denaturation at 95°C, 1 min annealing at 58°C, and 1 min extension at 72°C. PCR products were purified from 1.5–2% agarose gels by gel excision and elution by rapid centrifugation, followed by extractions with phenol, phenol/chloroform, and chloroform. DNA samples were ethanol precipitated and redissolved in 10 mM Tris·HCl (pH 7.4) and 1 mM EDTA. DNA concentrations were determined spectrophotometrically. The DNA used in the SFM analysis of the M.*Hha*I was amplified by PCR from plasmid pDE13 (27) to generate a 350-bp fragment with the *Hha*I site 204 bp from one end.

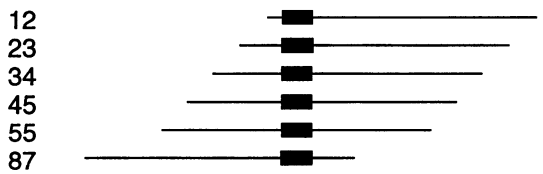

FIG. 2. DNA substrates used for circular permutation analysis of *Eco*RI DNA methyltransferase. Schematic shows the location of the *Eco*RI DNA methyltransferase binding site on each of the DNA fragments. The binding site (represented by the box) was moved from one end of the DNA to the other by annealing specific PCR primers onto plasmid pGem-3 to generate a set of fragments 110 bp long (see *Materials and Methods*).

Gel Mobility Shift Assays and Bend Angle Determination. Gel mobility shift experiments were performed with M.*Eco*RI and M.*Hha*I. The PCR fragments were radiolabeled with T4 polynucleotide kinase and [γ-^{32}P]ATP. Excess radiolabel was removed by gel filtration (25) using Bio-gel P-6 resin (Bio-Rad). Incubation reactions contained 1 nM DNA, 100 mM Tris·HCl (pH 8.0), 10 mM EDTA, 1 mM DTT, 10 μM sinefungin, and 5 nM M.*Eco*RI or 30 nM M.*Hha*I in a total volume of 40 μl. Binding reactions were incubated at 20°C for 1–5 min, loaded onto a 6% nondenaturing polyacrylamide gel, and run at 280 V for 2.5 h at 4°C. Following electrophoresis, the gels were dried and exposed to Fuji Medical x-ray film for 8–12 h.

Bend angle determination of gel shift experiments was done by the method of Thompson and Landy (26) using (*i*) intrinsically bent DNA standards of known bend angle and (*ii*) the empirical equation $\mu M/\mu E = \cos(\alpha/2)$, which relates the mobility of complexes formed with two DNA fragments having a binding site located at the center (μM) or near an end (μE). Plasmid constructs harboring between two and six phased A tracts were generously provided by Arthur Landy (Brown University). The plasmids were digested with *Nhe*I or *Bam*HI endonucleases to obtain fragments with A tracts located in the middle or at an end, respectively. The DNA standards were further treated with alkaline phosphatase and radiolabeled with T4 polynucleotide kinase and [γ-^{32}P]ATP.

SFM. DNA–protein complexes were observed in air by SFM with a Nanoscope III (Digital Instruments, Santa Barbara, CA) in tapping mode using Digital Instruments n^+ silicon tapping mode probes with a force constant of C = 40–100 N/m and a resonance frequency of n_o = 300–400 kHz (28). Binding reactions consisted of 3 nM DNA, 20 mM Hepes (pH 7.6), 1 mM DTT, and 30–50 nM M.*Eco*RI or 50–100 nM M.*Hha*I in a total volume of 10 μl. These concentrations were required to obtain significant numbers of protein–DNA complexes and do not lead to detectable enzyme binding to noncognate DNA (21, 22). Samples were incubated for 1–5 min at 20°C. The DNA was adhered to the mica surface by treatment with 1 μl of 100 mM $MgCl_2$ followed by gentle mixing. Samples were immediately deposited on freshly cleaved ruby mica (New York Mica, New York), washed with 15–20 drops of nanopure H_2O (Barnstead, Dubuque, IA), and excess liquid was blotted with filter paper and blown off with dry N_2 (g).

SFM Image Analysis. All samples were imaged at a scan rate of 1.8–2.2 lines/sec (512 × 512 points per image). The force exerted on the sample was minimized by retracting the tip just below the lift-off point. Images were taken without on-line filtering, and captured images were flattened to remove the background slope. Complexes for bend angle measurements all contained high features >4 nm in height at the center of the DNA fragment. For image analysis, images were enlarged, two tangential lines were drawn along the center of the protruding DNA arms on both sides of the protein, and the bend angle was measured. Bend angle measurements of DNA in the absence of protein was done as described (29). Statistical analysis and the generation of histograms was done using MATLAB (Mathworks, Natick, MA).

RESULTS AND DISCUSSION

Two assessments of DNA bending were used. The first approach utilized conventional gel retardation assays to detect and quantitate induced bending (26, 30). In the second approach, SFM provides direct visualization of protein–DNA complexes, allowing the assignment of bend angles and their distribution within a population (29, 31). DNA fragments of equivalent length containing a single *Eco*RI site located at varying distances from one end (Fig. 2) were used in a gel retardation-based circular permutation analysis (26, 30). Under the conditions of the experiments shown in Fig. 3, the DNA

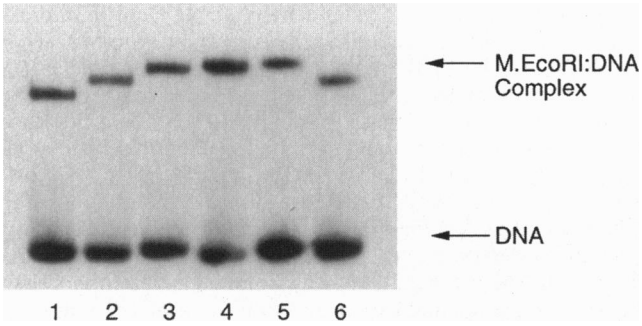

FIG. 3. Autoradiogram of circular permutation analysis of *Eco*RI DNA methyltransferase–DNA complexes. Binding reactions were done as described by using the DNA substrates shown in Fig. 2. The position-dependent effects on the migration of complexes are evident; the mobility decreases as the binding site is permuted from the end to the middle, as shown in lanes 1–5. Lane 6 represents a "duplicate" substrate of the DNA in lane 2; in this case the binding site is located the same distance from the opposite end.

is distributed between free and protein-bound forms and the protein–DNA complex involves a single enzyme bound per DNA molecule (21). The key feature of this assay is the variance in mobility of equi-length DNA fragments arising from alterations in their end-to-end distance (26, 30). An intrinsic or protein-induced bend at the center of a DNA fragment results in a decreased mobility relative to a fragment with a bend near an end. Circular permutation analysis of M.*Eco*RI demonstrated that the placement of the *Eco*RI site within each DNA fragment results in mobility differences of the protein–DNA complexes, which is a characteristic of bent DNA (Fig. 3, lanes 1–5) (26, 30).

To determine the magnitude of the bend angle, we followed the method described by Thompson and Landy (26). We constructed two DNA substrates of suitable length containing specifically placed *Eco*RI sites for comparison with a set of intrinsically bent DNA standards (26). Gel retardation experiments with M.*Eco*RI were performed (Fig. 4) and the bending angle (α) was determined by using (*i*) the bent DNA standards of known bend angle, and (*ii*) the empirical equation $\mu M/\mu E = \cos(\alpha/2)$, which relates the ratios of the mobilities of complexes formed with DNA fragments having a binding site located in the middle (μM) and near an end (μE). Measurements of DNA bending by these procedures were used to calculate bend angles of 54° ± 4° and 50° ± 2°, respectively.

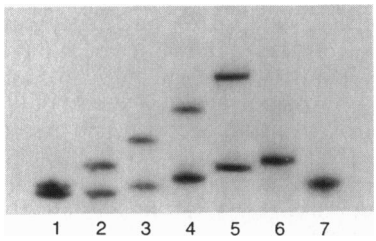

FIG. 4. Determination of bending angle induced by the *Eco*RI DNA methyltransferase by comparison to intrinsically bent A-tract DNA standards (26). *Eco*RI DNA methyltransferase–DNA binding conditions are the same as in Fig. 3. Lanes 1–5 contain the intrinsically bent DNA standards with the bent sequence located in the middle for the higher set of bands and at an end for the lower set of bands. Ratios of the migration positions of middle-to-end bent fragments were determined for each lane and used to generate a bend angle calibration plot (26). Complexes of the enzyme with 300-bp DNA fragments having a binding site either in the middle or at an end are shown in lanes 6 and 7, respectively. The ratio of the migration position of middle-bound to end-bound complexes in lanes 6 and 7 was determined and compared with the calibration plot obtained from the bending standards.

Anomalous electrophoretic behavior of protein–DNA complexes can be induced by changes in protein conformation rather than protein-induced DNA bending (32). Thus, to further characterize the apparent bending effects observed with the M.*Eco*RI, we used SFM to obtain images of M.*Eco*RI–DNA complexes. Enzyme–DNA complexes were prepared for SFM as described utilizing the same 300-bp DNA with the central *Eco*RI site used earlier (Fig. 4). The sample was prepared and deposited onto freshly cleaved ruby mica (33), and complexes were observed in air by SFM (29, 31). The resolution obtained in tapping mode provides facile discrimination between the DNA and the enzyme. Enzyme–DNA complexes are identified as high features at the expected location on the DNA (Fig. 5*A*). Many enzyme–DNA com-

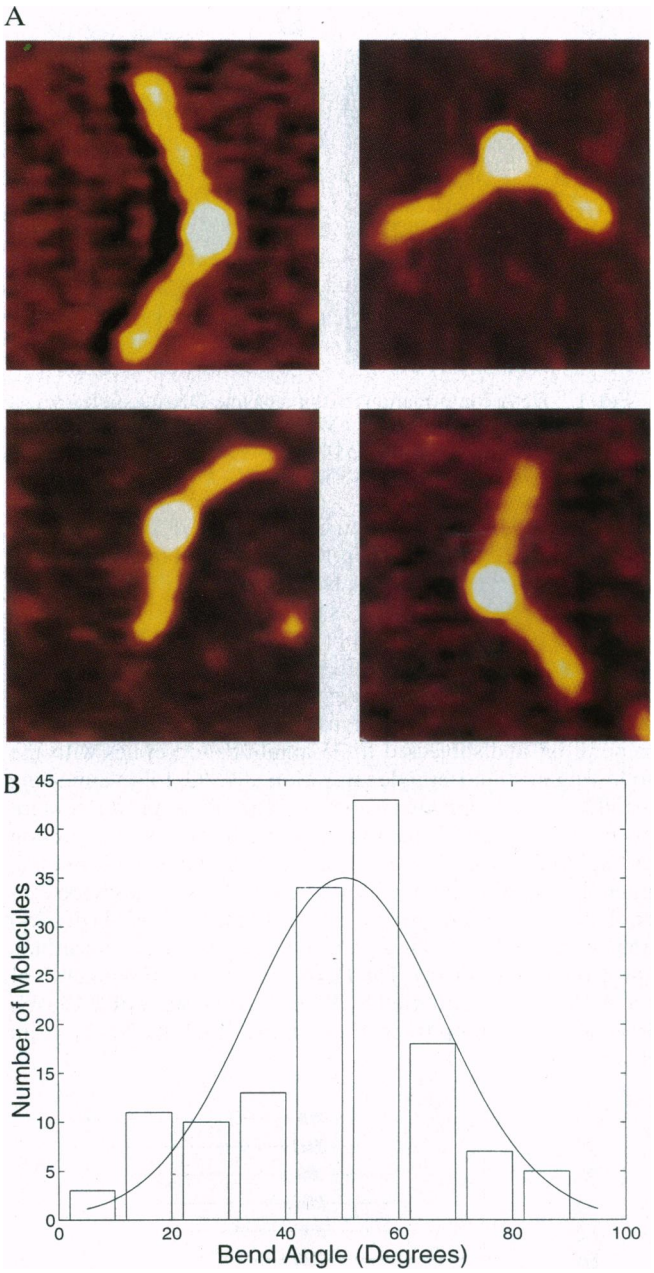

FIG. 5. (*A*) Enlarged SFM images of *Eco*RI DNA methyltransferase–DNA complexes showing the average measured bend angle of 51°. (*B*) Histogram of the measured bend angles for 144 complexes. Complexes for analysis were obtained from at least 10 separate depositions and were visualized at 1000–2000 nm scan sizes. Optimal binding and image quality observed by SFM yielded between 10–15% complexes with <1% bound nonspecifically.

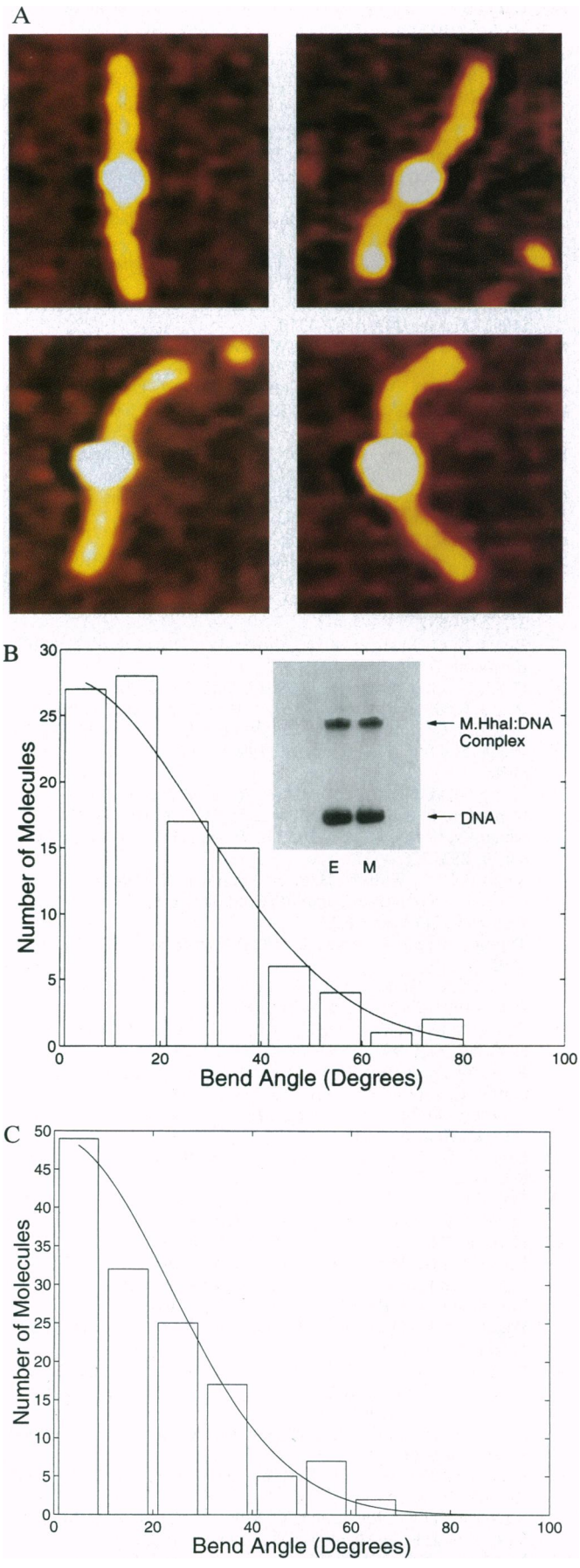

FIG. 6. (*A*) Enlarged SFM images of M.*Hha*I–DNA complexes showing the average measured bend angle of only 2°. (*B*) Histogram showing the measured bend angles for 100 complexes. The percentage of complexes visualized at 1000–2000 nm scan sizes was similar to that described for *Eco*RI DNA methyltransferase. (*Inset*) Gel shift with the *Hha*I DNA methyltransferase and DNA fragments containing a recognition site placed in the middle (M) and end (E). The similar mobilities suggest minimal bending is induced by the enzyme upon binding DNA. (*C*) Histogram showing 136 measurements of bend angles from depositions of DNA in the absence of protein. Free DNA bend angle assignment done as described (29) showed an average bend angle of 4° ± 23°.

plexes were analyzed to provide a statistically significant distribution of bend angles. Bend angle assignment of complexes was done according to the method described by Rees *et al.* (29), and Fig. 5*B* shows the histogram obtained from 144 individual measurements. The distribution is Gaussian with a mean bend angle (angle ± SD) of 51° ± 17°, in close agreement with that obtained by gel retardation (Fig. 4).

Inspection of other protein-DNA complexes (e.g., Fig. 1) shows that similarly bent DNA structures result in increased solvent exposure of base pairs within the DNA bend. Thus, the bent DNA conformation within the M.*Eco*RI–DNA complex may be important for sequence recognition and/or catalysis. The M.*Eco*RI reaction involves general acid-base catalysis (34), and methylation occurs directly at the poorly nucleophilic exocyclic amino group (35). Activation of the amino group may therefore be mediated by critical enzyme side chains which are only correctly assembled within the enzyme–bent DNA complex. Evidence that the bent DNA complex is functionally important comes from our analysis of a mutant M.*Eco*RI in which His-235 is replaced with an asparagine (R.A.G., M. Wyrsta, K. A. Maegley, and N.O.R., unpublished data). This enzyme does not bend DNA as revealed by the gel shift and SFM methods described for the wild-type enzyme. Interestingly, while the mutant's affinity for the specific site is decreased 40-fold, its affinity for nonspecific DNA is essentially unaffected. The decreased binding discrimination shown by this mutated methyltransferase is therefore correlated to an inability to bend DNA upon binding the cognate site. Further support for the functional requirement for DNA deformation by adenine methyltransferases comes from the recently solved crystal structure for the M.*Taq*I complexed with AdoMet (36). This complex shows that the bound AdoMet is significantly removed from the cleft suggested to bind DNA. The M.*Taq*I–AdoMet structure was recently used to predict that adenine DNA methyltransferases, like the cytosine C^5 DNA methyltransferases, are required to stabilize the target base in an extrahelical position (37, 38). We suggest that if the DNA bending detected for the M.*Eco*RI is generally true for adenine DNA methyltransferases, then the formation of a competent enzyme–DNA complex may require some combination of DNA bending, extrahelical base stabilization, or other, unidentified mechanisms. The recently described structure of the T4 endonuclease V-DNA complex clearly shows how a protein can significantly bend DNA while stabilizing an extrahelical base (39).

The cocrystal structure of the M.*Hha*I–DNA complex shows no significant DNA perturbation beyond the target cytosine (Fig. 1*D*; ref. 9). DNA bending by the M.*Hha*I was analyzed by SFM with 300-bp DNA fragments containing a centrally positioned recognition site. Mean representative SFM images are shown in Fig. 6*A*, and the histogram in Fig. 6*B* summarizes the analysis of measured complexes. The distribution is Gaussian, with a mean bend angle of 2° ± 28°. These values are similar to those observed with free DNA (Fig. 6*C*; 4° ± 23°), are consistent with the crystal structure (Fig. 1*D*; ref. 9), and are verified by the lack of any bending as shown by gel retardation analysis (Fig. 6*B inset*). Although the protein–DNA complexes with the M.*Hha*I all involved the expected,

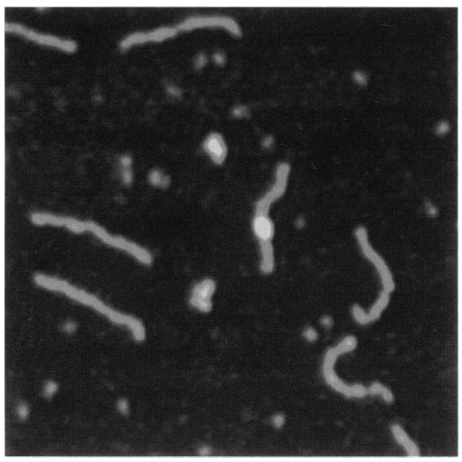

FIG. 7. SFM image showing another site-specific M.*Hha*I–DNA complex obtained with a 350-bp DNA fragment with the binding site located 204 bp from one end. The appearance of the enzyme "bump" clearly occurs at the expected location.

centrally located complex (Fig. 6*A*), we sought additional evidence that the lack of DNA bending was not due to nonspecific protein–DNA complexes. The formation of specific M.*Hha*I–DNA complexes was thus demonstrated with a 350-bp DNA fragment in which the recognition site was placed approximately three-fifths from one end; the enzyme is shown in Fig. 7 to bind in the predicted location along the DNA fragment.

The data provided here show that the M.*Eco*RI and M.*Hha*I clearly cause different distortions of DNA. Enhancing access to essential DNA moieties through localized DNA distortion may be a common feature among sequence-specific DNA modifying enzymes (40). As a subclass, AdoMet-dependent DNA methyltransferases have an additional requirement for such distortions. DNA methyltransferases are all required to position the methyl moiety of AdoMet proximal to a nucleophile within the target cytosine or adenine. Such a juxtaposition of DNA and AdoMet, in the absence of significant distortion of the DNA, would position the AdoMet molecule close to adjacent portions of the DNA or protein residues that determine sequence specificity. This presents a problem in that hundreds of methyltransferases that modify a large number of DNA sequences all use AdoMet in this fashion. The M.*Hha*I circumvents this dilemma by stabilization of the extrahelical cytosine, effectively reducing the reaction to the AdoMet-dependent methylation of a pyrimidine. While our results support the importance of DNA bending to sequence recognition with the M.*Eco*RI, the contribution of DNA bending toward increasing access to the target adenine remains uncertain.

We thank Dr. Karen Maegley for providing us with purified M.*Eco*RI and Dr. Sanjay Kumar for the generous gift of purified M.*Hha*I. We are grateful to Dr. Arthur Landy for providing us with the bending standards, Dr. Claudio Rivetti for the 350-bp DNA, Chip Walker for his assistance with the statistical analysis, and Amy Martin for her help with MIDAS graphics. We especially thank Mark Surby for his advice and insightful suggestions given throughout. This work was supported by grants from the National Science Foundation (MCB-9018474) and the American Cancer Society (JFRA-332) to N.O.R., and a Howard Hughes Undergraduate Research Fellowship and Pregraduate Mentorship Grant from the University of California Santa Barbara College of Letters and Science and the Dewolfe Undergraduate Research Fellowship from the Department of Chemistry, University of California, Santa Barbara to R.A.G.

1. Goodman, S. D. & Nash, H. A. (1989) *Nature (London)* **341,** 251–254.
2. Kahn, J. D. & Crothers, D. M. (1992) *Proc. Natl. Acad. Sci. USA* **89,** 6343–6347.
3. Shultz, S. C., Shields, G. C. & Steitz, T. A. (1991) *Science* **253,** 1001–1007.
4. Wu, H.-M. & Crothers, D. M. (1984) *Nature (London)* **308,** 509–513.
5. Parvin, J. D., McCormick, R. J., Sharp, P. A. & Fisher, D. E. (1995) *Nature (London)* **373,** 724–727.
6. Kim, Y., Geiger, J. H., Hahn, S. & Sigler, P. (1993) *Nature (London)* **365,** 512–520.
7. Kim, J. L., Nikolov, D. B. & Burley, S. K. (1993) *Nature (London)* **365,** 520–527.
8. Wing, R., Drew, H., Takano, T., Broka, C., Tanaka, S., Itakura, K. & Dickerson, R. E. (1980) *Science* **287,** 755–758.
9. Kim, Y., Grable, J. C., Love, R., Greene, P. J. & Rosenberg, J. M. (1991) *Science* **249,** 1307–1310.
10. Winkler, F. K., Banner, D. W., Oefner, C., Tsernoglou, D., Brown, R. S., Heathman, S. P., Bryan, R. K., Martin, P. D., Petratos, K. & Wilson, K. S. (1993) *EMBO J.* **12,** 1781–1795.
11. Klimasauskas, S., Kumar, S., Roberts, R. J. & Cheng, X. (1994) *Cell* **76,** 357–369.
12. Mol, C. D., Kuo, C., Thayer, M. M., Cunningham, R. P. & Trainer, J. A. (1995) *Nature (London)* **374,** 381–386.
13. Savva, R., McAuley-Hecht, K., Brown, T. & Pearl, L. (1995) *Nature (London)* **373,** 487–493.
14. Borman, S. (1995) *Chem. Eng. News* **73,** 9.
15. Posfai, J., Bhagwat, A. S., Posfai, G. & Roberts, R. J. (1989) *Nucleic Acids Res.* **17,** 2421–2435.
16. Malone, T., Blumenthal, R. M. & Cheng, X. (1995) *J. Mol. Biol.* **253,** 618–632.
17. Reich, N. O., Maegley, K. A., Shoemaker, D. & Everett E. (1991) *Biochemistry* **30,** 2940–2946.
18. Reich, N. O. & Everett E. (1990) *J. Biol. Chem.* **265,** 8929–8934.
19. Wu, J. C. & Santi, D. V. (1987) *J. Biol. Chem.* **262,** 4778–4786.
20. Reich, N. O. & Mashhoon, N. (1991) *Biochemistry* **30,** 2933–2939.
21. Reich, N. O. & Mashhoon, N. (1990) *J. Biol. Chem.* **265,** 8966–8970.
22. Surby, M. & Reich, N. O. (1996) *Biochemistry* **35,** 2201–2208.
23. Renbaum, P. & Razin, A. (1992) *FEBS Lett.* **313,** 243–247.
24. Reich, N. O., Olsen, C., Osti, F. & Murphy, J. (1992) *J. Biol. Chem.* **252,** 7265–7272.
25. Sambrook, J., Fritsch, E. F. & Maniatis, T. (1989) *Molecular Cloning: A Laboratory Manual* (Cold Spring Harbor Lab. Press, Plainview, NY), 2nd Ed.
26. Thompson, J. F. & Landy, A. (1988) *Nucleic Acids Res.* **16,** 9687–9705.
27. Erie, D. A., Hajiseyedjavadi, O., Young, M. C. & von Hippel, P. H. (1993) *Science* **262,** 867–873.
28. Bustamante, C., Vesenka, J., Tang, C. L., Rees, W., Guthold, M. & Keller, R. (1992) *Biochemistry* **31,** 22–26.
29. Rees, W. A., Keller, R. W., Vesenka, J. P., Yang, G. & Bustamante, C. J. (1993) *Science* **260,** 1646–1649.
30. Crothers, D. M., Gartenberg, M. R. & Schrader, T. E. (1991) *Methods Enzymol.* **208,** 118–146.
31. Erie, D. E., Yang, G., Shultz, H. C. & Bustamante, C. (1994) *Science* **266,** 1562–1566.
32. Gartenberg, M. R., Ampe, C., Steitz, T. A. & Crothers, D. M. (1990) *Proc. Natl. Acad. Sci. USA* **87,** 6034–6038.
33. Hansma, H. G., Sinsheimer, R. L., Groppe, J., Bruice, T. C., Elings, V., Gurley, G., Bezanilla, M., Mastrangelo, I. A., Hough, P. V. C. & Hansma, P. K. (1993) *Scanning* **15,** 296–299.
34. Mashhoon, N. & Reich, N. O. (1994) *Biochemistry* **33,** 7113–7119.
35. Pogolotti, A., Ono, A., Subramaniam, R. & Santi, D. (1988) *J. Biol. Chem.* **263,** 7461–7464.
36. Labahn, J., Granzin, J., Schluckebier, G., Robinson, D. P., Jack, W. E., Schildkraut, I. & Saenger, W. (1994) *Proc. Natl. Acad. Sci. USA* **91,** 10957–10961.
37. Schluckebier, G., O'Gara, M., Saenger, W. & Cheng, X. (1995) *J. Mol. Biol.* **247,** 16–20.
38. Malone, T., Blumenthal, R. M. & Cheng, X. (1995) *J. Mol. Biol.* **253,** 618–632.
39. Yassylyev, D. G., Kashiwagi, T., Mikami, Y., Ariyoshi, M., Iwai, S., Ohtsuka, E. & Morikawa, K. (1995) *Cell* **83,** 773–782.
40. McClarin, J. A., Frederick, C. A., Wang, B.-C., Greene, P., Boyer, H. W. & Rosenberg, J. M. (1986) *Science* **234,** 1526–1541.